ChemPubSoc Europe

DOI: 10.1002/chem.201801165

CHEMISTRY
A European Journal
Full Paper

Flow Reactions

High Throughput Experimentation and Continuous Flow Validation of Suzuki–Miyaura Cross-Coupling Reactions

Zinia Jaman,[a] Ahmed Mufti,[b] Samyukta Sah,[a] Larisa Avramova,[a] and David H. Thompson*[a]

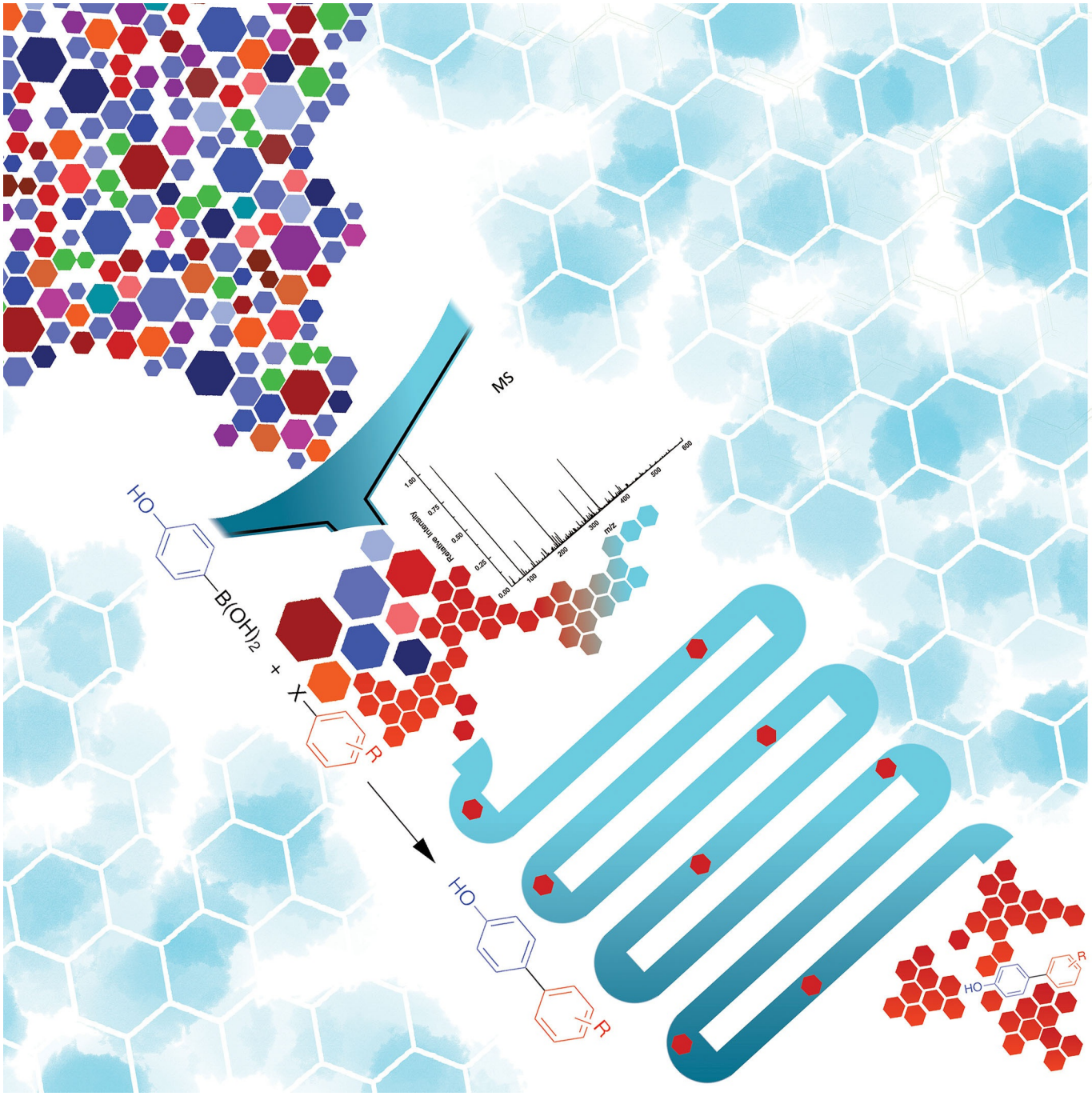

© 2018 Wiley-VCH Verlag GmbH & Co. KGaA, Weinheim

Abstract: Traditional methods to discover optimal reaction conditions for small molecule synthesis is a time-consuming effort that requires large quantities of material and a significant expenditure of labor. High-throughput techniques are a potentially transformative approach for reaction condition screening, however, rapid validation of the reaction hotspots under continuous flow conditions remains necessary to build confidence in high throughput screening hits. Continuous flow technology offers the opportunity to upscale the screening hotspots and optimize their output of the target compounds due to the exceptional heat and mass transfer ability of flow reactions that are conducted in a smaller and safer reaction volume. We report a robotic high throughput technique to execute reactions in multi-well plates that were coupled with fast mass spectrometric analysis using an autosampler to accelerate the reaction screening process. Palladium-catalyzed Suzuki–Miyaura cross-coupling reactions were screened in this system and a heat map was generated to identify the best reaction conditions for downstream scale-up under continuous flow. Here, high throughput experimentation reactions in 96-well plates were performed for 1 h at 50 °C, 100 °C, 150 °C, and 200 °C before diluting them into 384-well plates for mass analysis. With the aid of high throughput tools, 648 unique experiments were conducted in duplicate. The cross-coupling reactions were evaluated as a function of stoichiometry, temperature, concentration, order of addition, and substrate type. The hotspots from high throughput experimentation were examined using a microfluidic Chemtrix system that confirmed the positive reaction leads as true positives. Negative outcomes identified by these experiments were found to be true negatives by microfluidic reaction evaluation. Quantitation of product yields was performed using high-performance liquid chromatography-mass spectrometry (HPLC/MS-MS).

Introduction

The development of automated high throughput experimentation (HTE) methods has been shown to boost lab productivity by rapid generation of comprehensive reaction data that enriches our understanding of reaction scope and limitations.[1] HTE across a range of settings have impacted many areas of biology, drug discovery, medicinal chemistry,[2] and catalysis.[4] Automated reactions can often be run in parallel, but the downstream analysis is typically a bottleneck due to relatively slow chromatographic separation and/or quantitation methods. HTE coupled with rapid mass spectrometry (MS) analysis can accelerate both the discovery and optimization of reaction conditions, particularly in the cases of chemical process development[3a,4] and (bio)pharmaceutical drug development where pressures to shorten the time to market are increasing.[5] HTE has been challenging in the case of organic reaction optimization, especially for catalytic reactions that may employ solid catalysts or volatile organic solvents.[3b,4a]

The central goal in HTE for reaction optimization is the discovery of the best experimental conditions for a given set of precursors to identify the most prominent reaction hotspots. After HTE, a quick validation of these hotspots is used to build confidence in the reaction hits identified by the HTE process. Microfluidic reaction evaluation of the HTE hits are an essential step for validating organic transformations[6] under continuous flow conditions. This has been shown to be especially true for catalytic reactions that can be achieved under faster and greener conditions.[7] Moreover, fast microfluidic synthesis of small organic molecules, coupled with continuous reaction monitoring using electrospray ionization mass spectrometry (ESI-MS), shows even greater promise for rapid optimization of continuous production methodology.[8] Here, we report a study of the Suzuki–Miyura (S-M) cross-coupling reaction as a test bed for HTE reaction optimization using ESI-MS as a readout tool. The S-M reaction was chosen because carbon-carbon bond formation via palladium-catalyzed S-M cross-coupling is an important reaction for small molecule synthesis[9] that has been widely used.[10] Recently Perera et al. and Santanilla et al. have reported[3b,6] high throughput S-M cross-coupling reactions in both flow and batch mode with demonstration of the ability to screen reactions quickly on the nanomole-scale under different conditions. These efforts encouraged us to explore the S-M cross-coupling reactions in the synthesis of precursor compounds of importance in biological, pharmaceutical, and materials applications.

A simple and efficient technique for identifying and optimizing S-M reaction conditions with different functional group tolerance is described. Important biphenyl intermediates (Figure 1) were synthesized using S-M cross-coupling reactions without protecting the functional groups. Our HTE effort was focused on identifying the preferred reaction parameters that would enable faster optimization of microfluidic reactions by eliminating failed reaction conditions from the flow chemistry search process. Decreasing the number of unsuccessful transformations will focus efforts on the rapid discovery of compound leads whose syntheses are more robust and economical in a shorter period of time.

[a] *Z. Jaman, S. Sah, L. Avramova, Prof. D. H. Thompson*
Department of Chemistry, Bindley Bioscience Centre
Purdue University
1203 W State St
West Lafayette, IN 47906 (USA)
E-mail: davethom@purdue.edu

[b] *A. Mufti*
School of Chemical Engineering
Purdue University
480 W Stadium Ave
West Lafayette, IN 47907 (USA)

Supporting information and the ORCID identification number(s) for the author(s) of this article can be found under:
https://doi.org/10.1002/chem.201801165.

© 2018 Wiley-VCH Verlag GmbH & Co. KGaA, Weinheim

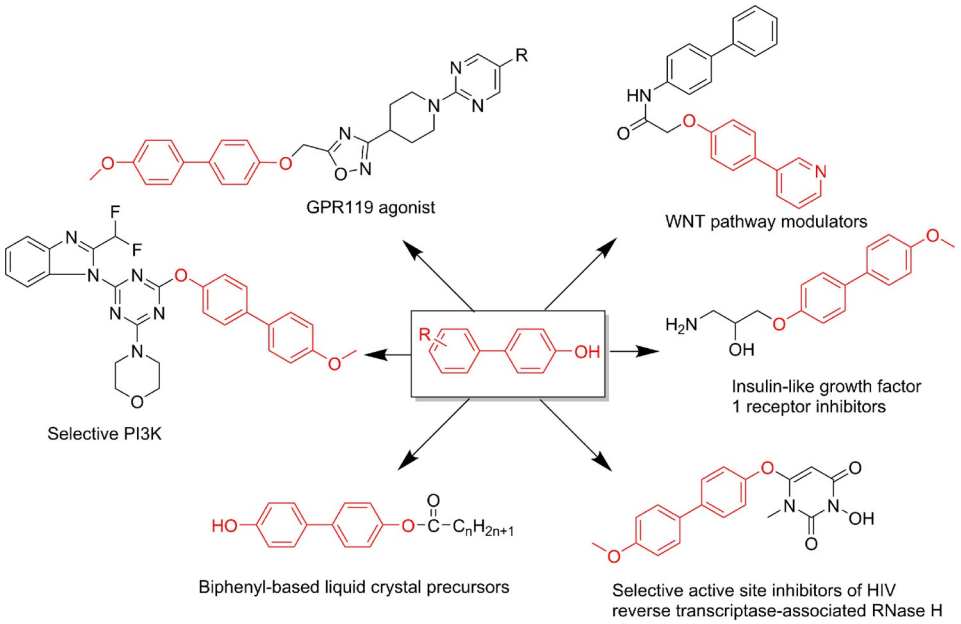

Figure 1. [1,1′-Biphenyl]-4-ol synthon and its use in some important biological, pharmaceutical, and materials science target compounds.

The S-M reaction has already been reported under some limited ranges of flow conditions,[7,11] nonetheless, we explored its utility toward the synthesis of important synthons[12] in a microfluidic reactor using EtOH as solvent to broadly explore the utility of this transformation.[7,10c]

Automated HTE of S-M reactions was performed in 96-well plates using 4-hydroxyphenylboronic acid and 11 different aryl halides (Scheme 1) with order of addition, stoichiometry, temperature, and concentration as independent variables. These experiments led to the discovery of optimized batch conditions from hundreds of different reaction conditions using XPhosPdG3 as catalyst and 1,8-diazabicyclo[5.4.0]undec-7-ene (DBU) as the base. Small scale microfluidic reactions employing the best conditions from the batch reaction screening produced up to 98% yield of S-M coupled products by HPLC/MS-MS analysis, thus validating our findings from HTE.

Results and Discussion

High Throughput Experimentation: A high-precision Biomek FX robot was used for the preparation of nanoliter scale reaction mixtures for automated HT screening of S-M reaction conditions with downstream MS analysis. The reactions were performed in glass vials sealed within four 96-well aluminum blocks and the outcome monitored with a highly sensitive triple quadrupole MS coupled to an autosampler for rapid determination of the reaction product distribution. Full mass spectra in negative ion mode were recorded for each reaction mixture.

The S-M cross-coupling reactions were evaluated in EtOH using 4-hydroxyphenylboronic acid (**1**), various aryl halides, and XPhosPdG3 as palladium catalyst (Scheme 1), to explore the impact of different aryl halide substrates on reaction efficiency without the use of additional protection/deprotection steps. Reaction mixtures (45 μL of total volume of each well) were deposited in duplicate within four 96 glass-lined Al well plates and the reactions heated at either 50, 100, 150, or 200 °C for 1 h before quenching to 20 °C, centrifuging, and diluting into 384 well plates for MS analysis. Each square in Figure 2 represents a unique reaction condition. The first two columns and last four columns are negative controls. Although the ionization efficiencies vary for each compound, the outcomes are reported based on reaction product peak intensity to enable a simple and uniform comparison (see Supporting Information for details).

Our initial HTE experiments explored the S-M reaction by adding in sequence a mixture of **1**, base, and catalyst solution in EtOH, followed by aryl halide (**2**–**12**) addition. Unfortunately, no product peak was detected in MS, although a prominent peak corresponding to the hydrolyzed boronic acid product was observed. These findings suggest that the catalyst was poisoned by the base while sitting idle at 20 °C during subsequent robotic reagent transfers over the intervening period (20 min) before the reaction was initiated by heating. When the order of addition was changed to aryl halide and **1**, followed by base and catalyst in sequence, the product peak was observed in the resulting MS, although the product yields were not satisfactory (Figure 2, top). We attribute these finding to the consumption of **1** by base before catalyst addition such that insufficient boronic acid was available to participate in the catalytic cycle. This hypothesis was further supported by the observation of predominantly product ions in the MS under conditions of excess boronic acid (e.g., at 20:1–2:1 stoichiometries). Nonetheless, when the base solution was added after the catalyst, a significant increase in product conversion was observed (Figure 2, bottom), with the accompanying detection of self-coupled **1**-**1** product by MS (see Supporting Information for detail results).

© 2018 Wiley-VCH Verlag GmbH & Co. KGaA, Weinheim

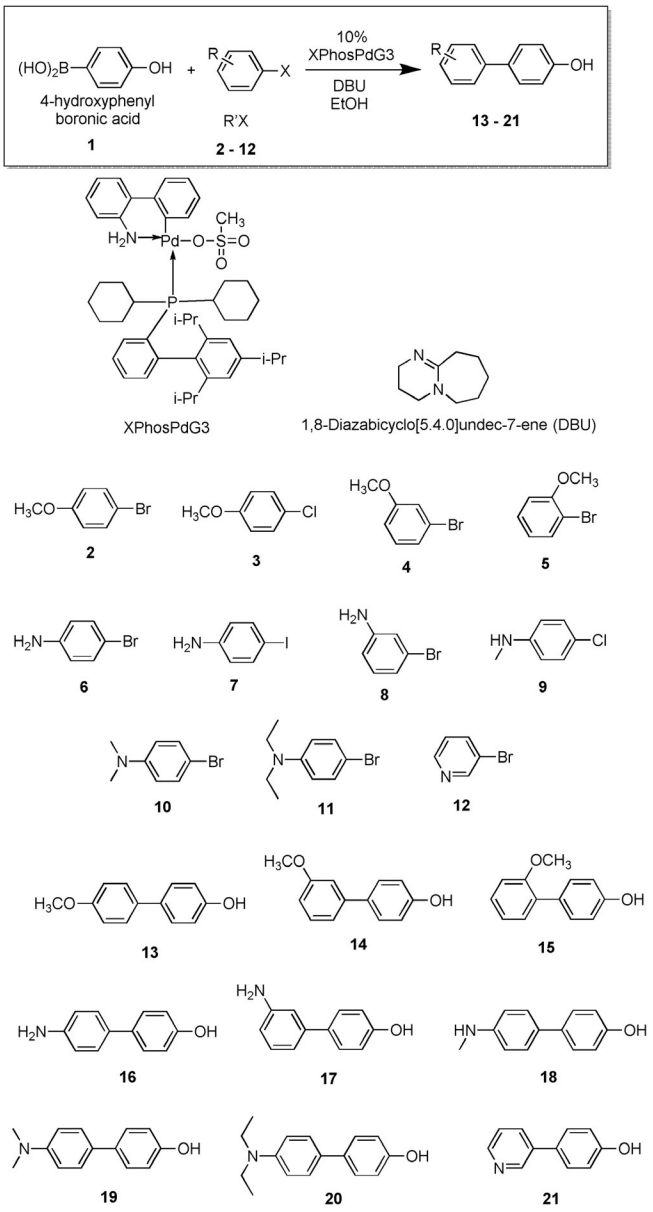

Scheme 1. Substrate scope evaluated in high-throughput experimentation of S-M cross-coupling reactions to generate various biphenyl products.

We subsequently utilized the optimal conditions identified in Figure 2 for a broader screen of aryl halide substrates. Our results show that both electron-rich and electron-deficient aryl halides (**2**–**12**) were tolerated to produce cross-coupled products in moderate to good yield as assessed by product peak intensities (Figure 3 A–D). Comparison of the anisole family of precursors (**2**–**5**) revealed that the *meta*-positioned methoxy group (**4**, Figure 3 C) provided more desired product than *ortho* (**5**, Figure 3 D) or *para* (**2**&**3**, Figure 3 A&B) due to the reduced electron donating contribution from the *meta* placement of this substituent.[13]

Haloanilines (**6**–**11**) were also transformed into the corresponding biphenyl products, yielding moderate peak intensities for the cross-coupled products (Figure 4 A–G). As seen in the anisole family of compounds, the *meta* product, **17** (**1** + **8**, Figure 4 C), produced a higher peak intensity than *para*, **16** (**1** + **6**/**7**, Figure 3 A&B), for the primary amine substrates. When aniline- and anisole-derived products were compared, higher product peak intensities were observed for the anisole family of compounds, **13**–**15** than the anilines series, **16**–**20** (Figures 3 and 4). We attribute these finding to the greater electron donating property of the amine versus methoxy substituents such that formation of the aminophenyl palladium intermediate is less favorable in the rate limiting oxidation addition step of the catalytic cycle in the aniline series.

The product peak intensities for secondary and tertiary substrates were higher than those observed for the primary amines (Figure 4 A–C vs. Figure 4 D–F), consistent with the observation that primary amines are known to more readily coordinate with palladium catalysts than secondary or tertiary amines due to steric hindrance.[14] In the case of the pyridine derivative, a higher product peak intensity was observed due to the comparative electron deficiency of the pyridine ring relative to the aniline series (**1** + **12**, Figure 4 G vs. Figure 4 A–F; see Supporting Information for detail results).

Figure 5 shows the product peak intensities for 504 unique Suzuki–Miyaura reactions, employing one of 11 different aryl halides and 4-hydroxyphenyl boronic acid in the presence of DBU and 10% XPhosPdG3. Since some low level peak intensities were observed in the negative control reactions that we attributed to noise during acquisition of the MS data, we used $>50\%$ peak intensity as the selection criterion to choose reaction hotspots in this map for subsequent evaluation in a series of microfluidic reactions.

Microfluidic evaluation of HT experimentation leads

After identifying reaction hotspots from the HTE campaign, we proceeded to test one of the favorable conditions for each reaction to determine the confidence level that could be assumed for the two different reaction formats (i.e., batch 96-well vs. continuous flow). For all microfluidic reactions, the reactions employing a 1:1 ratio of 4-hydroxyphenylboronic acid and aryl halide were evaluated for 0.5, 1, 3 and 6 min residence times at either 100 or 150 °C. Reactions using 10% XPhosPdG3 catalyst loadings were complicated by chip clogging problems shortly after initiating the reaction (see Supporting Information for details). This problem was obviated by reducing the catalyst loading to 0.5% since prior work has shown that S-M transformations are more efficient in continuous flow than under traditional bulk reaction conditions due to superior mass and heat transfer and greater mixing efficiency in the narrow reactor channels. The order of addition did not matter in the microfluidic synthesis since all the reagents come into contact within the same mixing region (Figure 6). The formation of the expected products was confirmed by TLC and MS. As the data in Figure 7 show, the results from microfluidic continuous reactions were comparable to the findings from bulk screening.

The data in Figure 7 shows that the S-M reaction tolerates electron donating substitutes in the aryl halide substrate to

© 2018 Wiley-VCH Verlag GmbH & Co. KGaA, Weinheim

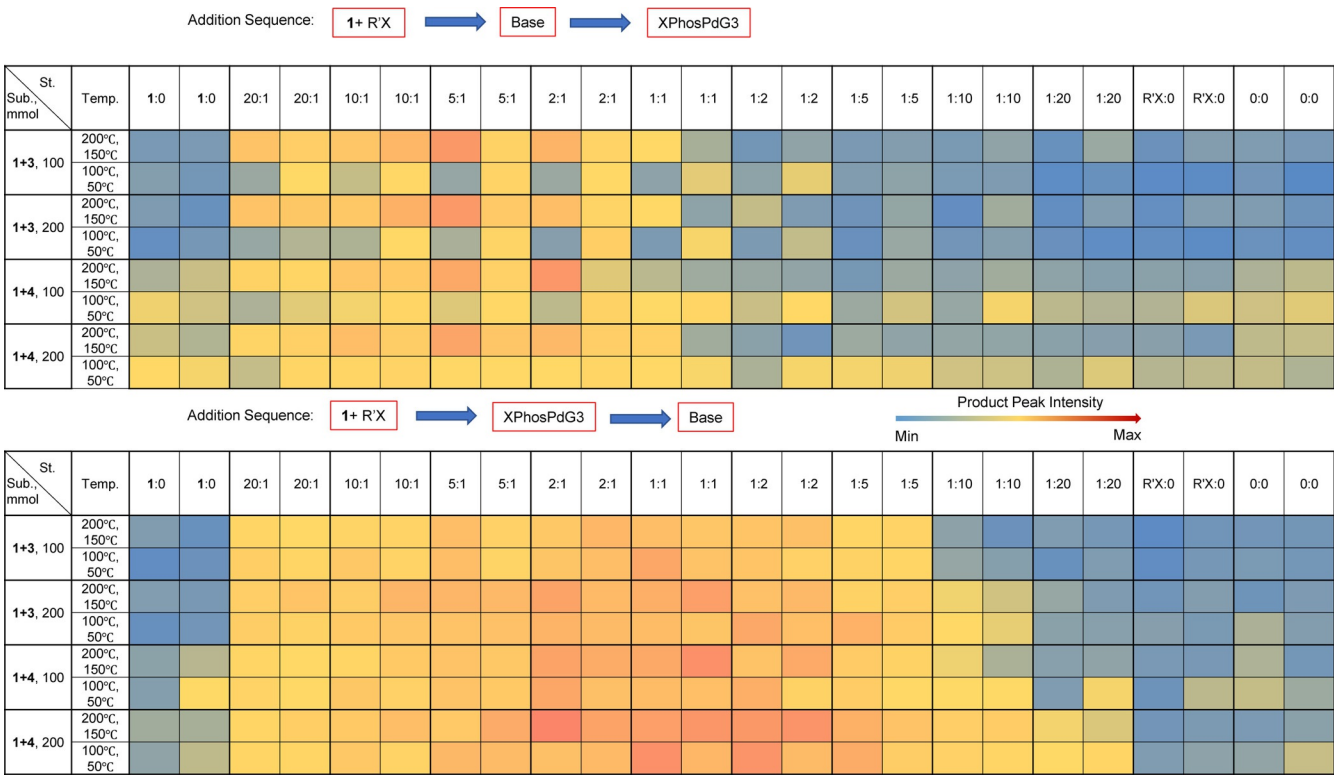

Figure 2. HT reaction outcomes as a function of reagent addition order and substrate concentration in the reaction mixture. Each quantity is an average of two experimental measurements. Each set of similar substrates and stoichiometries appears as a set of four conditions wherein the top left, top right, bottom left and bottom right entries are reactions run at 200 °C, 150 °C, 100 °C and 50 °C, respectively. The first two columns (St. = **1**:0) and last four columns (St. = R'X:0 and 0:0) are the negative controls. Sub = substrates; St = stoichiometry.

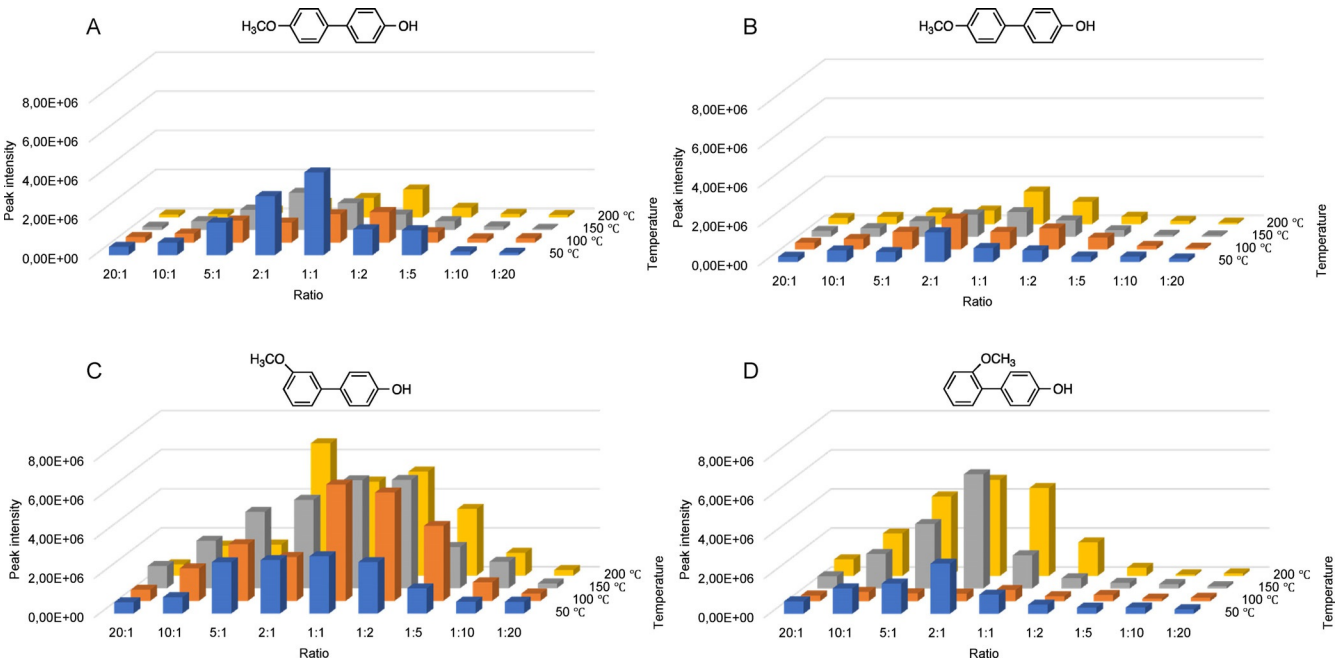

Figure 3. Comparative coupling efficiencies for anisole-type biphenyl products formed under different temperature and stoichiometric conditions. Reactant concen- trations were 200 mmol, except for **1** + **5** that was run at 100 mmol, 400 mmol DBU, and 10% XPhosPdG3. A = **1** + **2**; B = **1** + **3**; C = **1** + **4**; D = **1** + **5**.

afford the cross coupled products with varying efficiency. In both bulk and microfluidic experiments, *meta* (**1** + **4**) directed anisole biphenyl products showed higher product conversion than *ortho* (**1** + **5**), but in continuous flow processes, *para* (**1** + **2** & **1** + **3**) also showed higher product peak intensities (Figure 4 and 7). Similarly, bulky tertiary amine (**1** + **9**) and pyri-

© 2018 Wiley-VCH Verlag GmbH & Co. KGaA, Weinheim

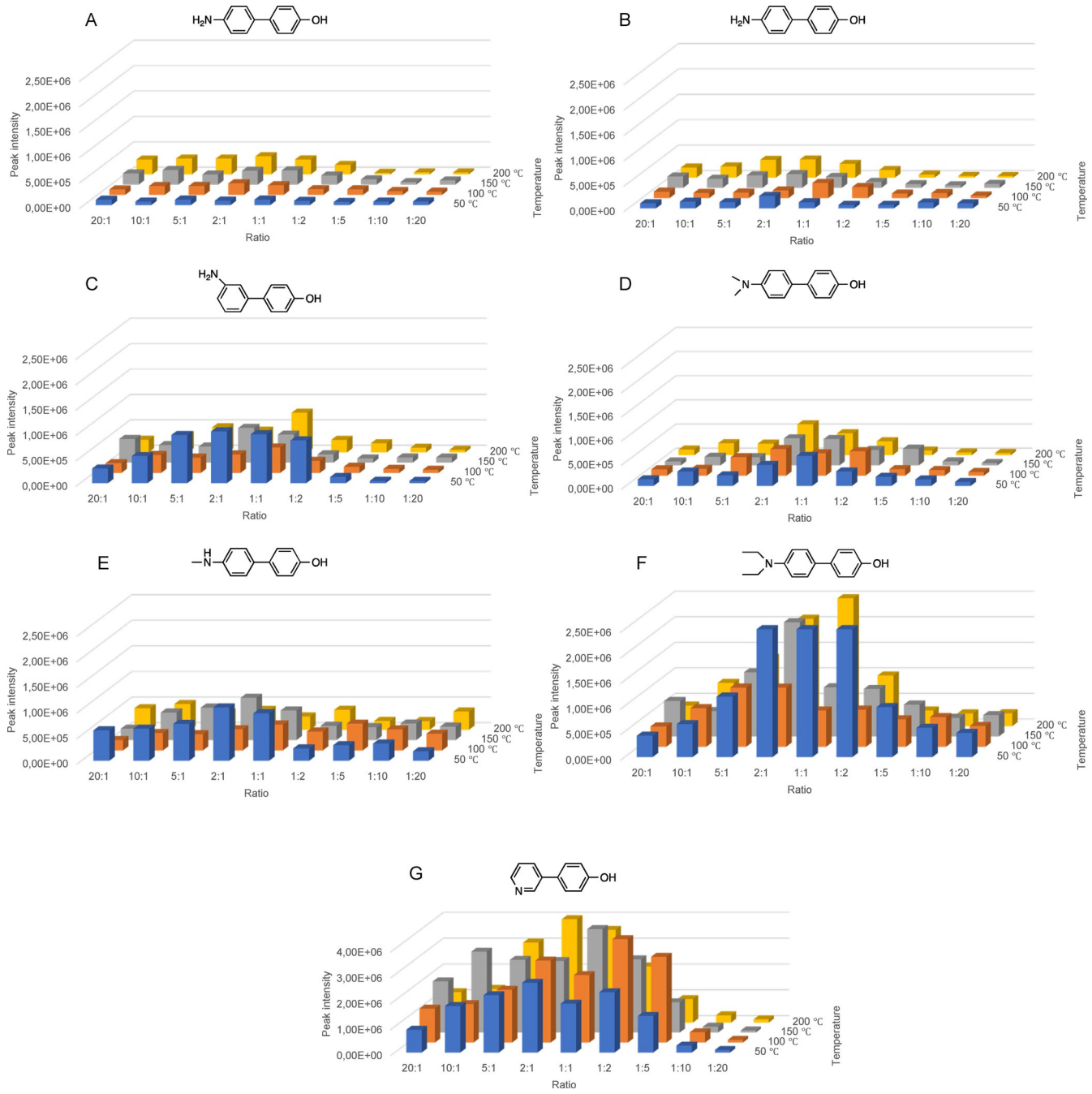

Figure 4. Comparative coupling efficiencies for aniline-type biphenyl products formed under different temperature and stoichiometric conditions. Reactant concentrations were 200 mmol, 400 mmol DBU, and 10% XPhosPdG3. A = **1** + **6**; B = **1** + **7**; C = **1** + **8**; D = **1** + **10**, E = **1** + **9**, F = **1** + **11**, G = **1** + **12**.

dine (**1** + **12**) precursors generated higher product peak intensities in both the bulk screening and flow synthesis formats.

We also investigated the negative results obtained from HTE and evaluated those reaction conditions under continuous flow (Figure 8). In both cases, almost no product peak was observed, even at extended residence times (e.g., 15 min at 150 °C in the case of **1** + **8**).

Next, we focused on testing the validity of using product ion intensities as a measure of reaction progress. The anisole and pyridine reaction products were selected for evaluation by HPLC/MS-MS since these products showed high peak intensities in both bulk screening and microfluidic reactions. A general trend of increasing product yield was observed for all anisoles (**2**–**5**) and pyridine **12** starting materials (Table 1). High yields were observed for **14** and **21** as was expected from the screening results. In most cases, there was good agreement between peak intensities and quantitative product yield. A low yield for **15** was observed due to the steric demands of the *o*-MeO substituent that requires more energy to drive the reaction.[12e, 13]

© 2018 Wiley-VCH Verlag GmbH & Co. KGaA, Weinheim

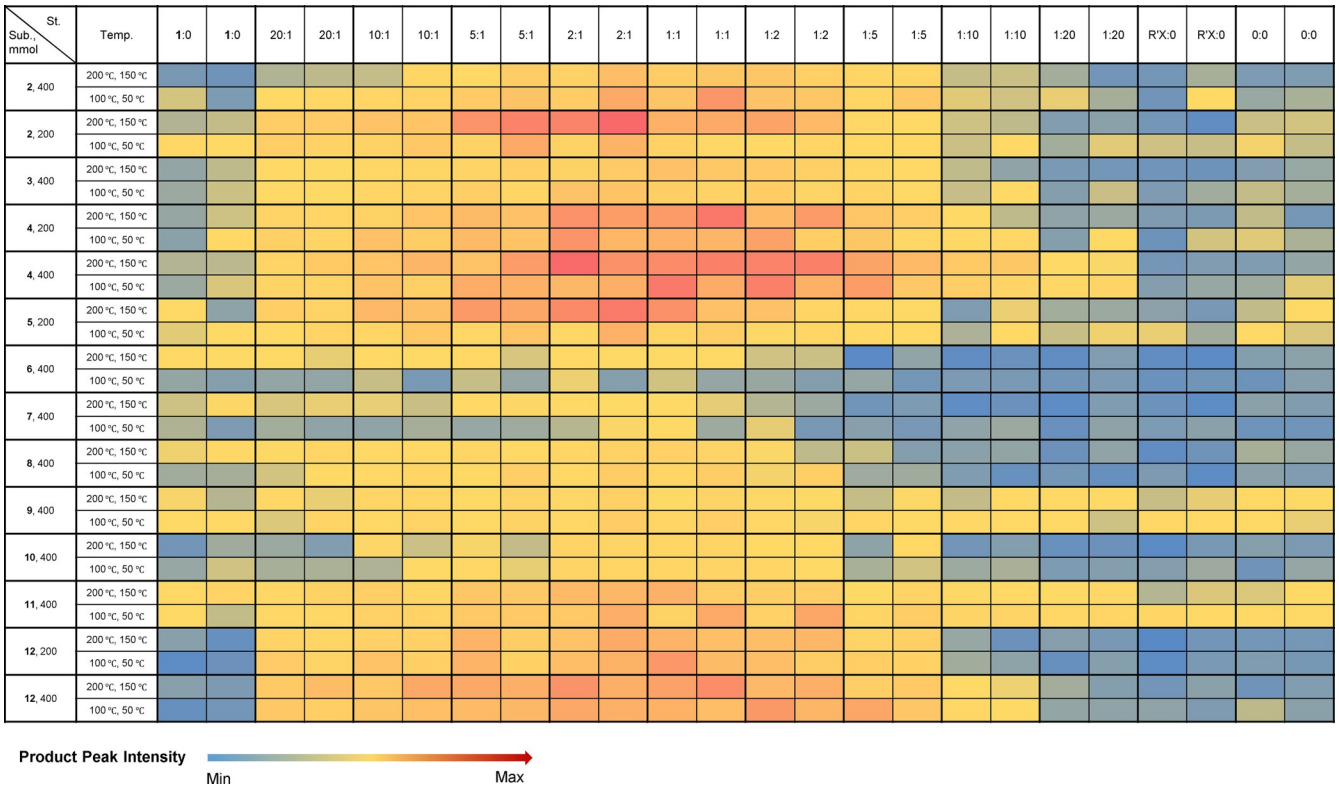

Figure 5. Product peak intensities observed for 504 unique S-M reactions run in bulk mode with the order of addition of base solution after the catalyst. Each quantity is an average of two experimental measurements. The product peak intensity data is normalized across the entire matrix. Each row indicates reactions of nine ratios of substrates including the control reactions at two different temperatures. Each set of similar substrates and stoichiometries appears as a set of four conditions, wherein the top left, top right, bottom left and bottom right entries are reactions run at 200, 150, 100 and 50 °C, respectively (see Supporting Information for details). The first two columns (St. = 1:0) and last four columns (St. = R'X:0 and 0:0) are the negative controls. Sub = substrates; St = stoichiometry.

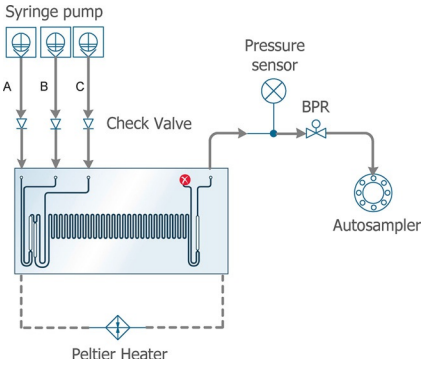

Figure 6. Chemtrix reactor and fluid handling for continuous flow synthesis of S-M cross coupling reactions. A = 1:1 mixture of 4-hydroxyphenylboronic acid and aryl halide; B = DBU, C = XPhosPdG3.

Conclusions

This investigation explored the use of a robotic HTE technique to execute reactions in 96-well arrays that were subsequently coupled with fast MS analysis using an autosampler. Palladium catalyzed S-M cross-coupling reactions were screened in this system to generate a heat map of reactivity to inform conditions for the downstream scale up in continuous flow. A total of 648 unique experiments using 4-hydroxyphenylboronic acid and 11 different aryl halides were explored in duplicate and the results reported as a function of MS peak intensity. The comparison of some successful reactions from HTE were run under microfluidic conditions; these experiments confirmed that the positive conditions identified by HTE were true positives. Furthermore, negative reaction conditions identified by this method also produced negative results under microfluidic conditions, even after long residence times at higher temperature. Moreover, quantitative analysis by HPLC/MS-MS provided evidence of a good correlation between HT reaction screening and microfluidic reactions.

This HTE and microfluidic validation approach may be equally applicable to other catalytic and noncatalytic reactions to rapidly reveal vast reactivity landscapes to guide reaction optimization efforts. This method might also be applied to the identification of optimal conditions for challenging substrates or the discovery of new routes for the production of bioactive molecules. Further investigation along these lines will be needed to assess the robustness of this correlation.

Experimental Section

All chemicals and reagents were purchased from Sigma–Aldrich (St. Louis, MO) and used without purification. All standards for quantitation were purchased from Combi-Blocks, Inc. (San Diego, CA).

© 2018 Wiley-VCH Verlag GmbH & Co. KGaA, Weinheim

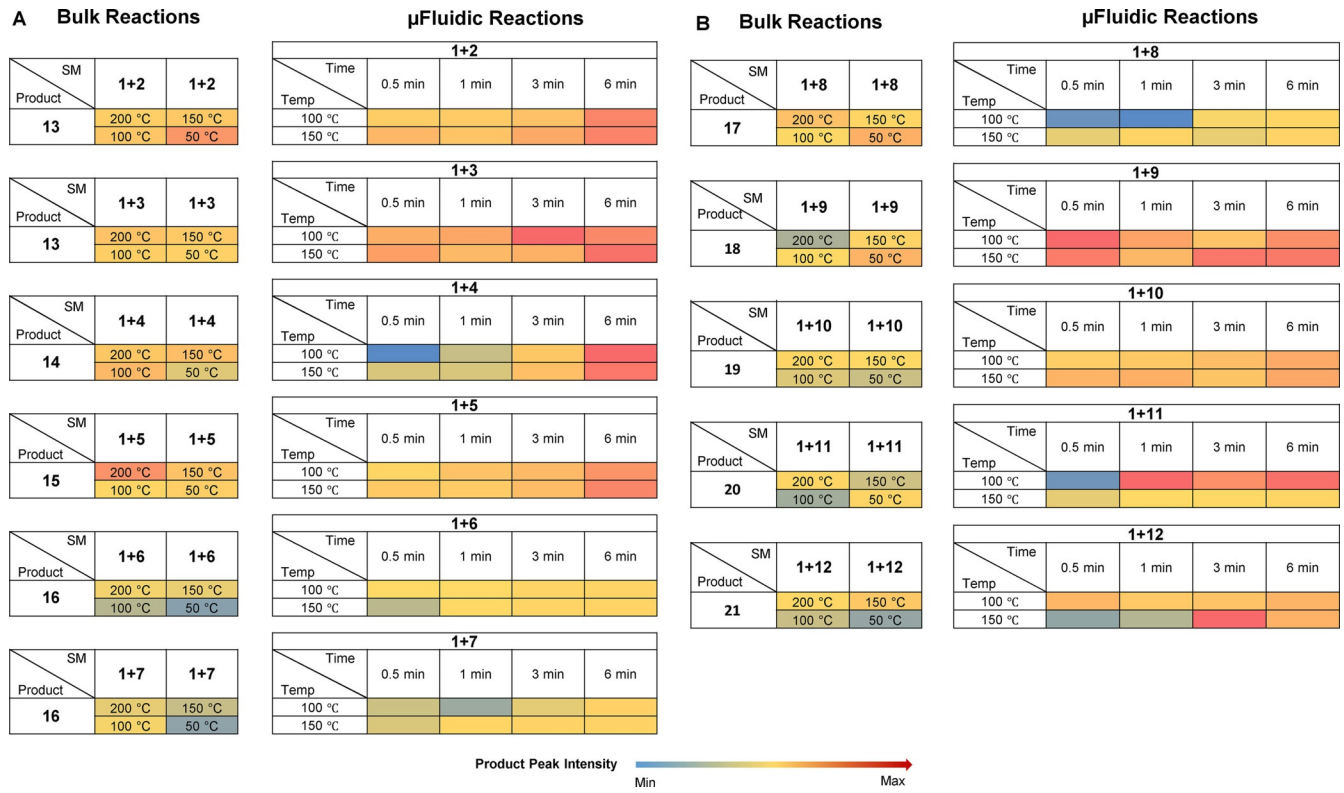

Figure 7. Comparison of microfluidic and bulk screening outcomes for S-M reactions performed under similar conditions using 200 mmol substrate loading and a 1:1 4-hydroxyphenylboronic acid:aryl halide stoichiometry.

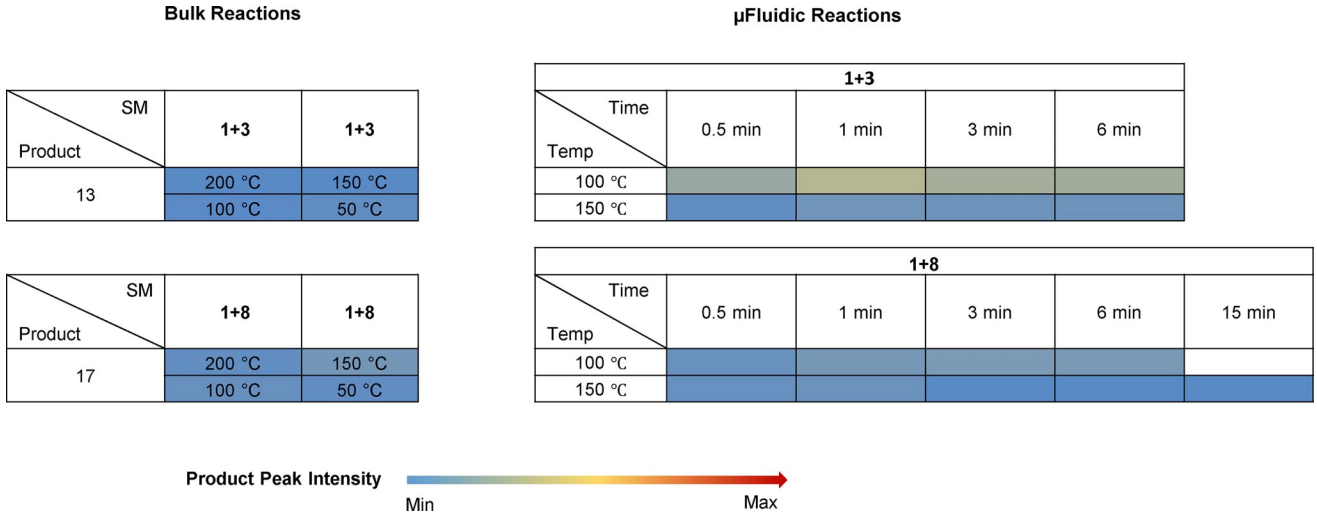

Figure 8. Comparison of microfluidic and bulk screening outcomes for S-M reactions that gave negative bulk reaction results. The same reaction conditions were used in each case with 200 mmol substrate loading and 1:20 4-hydroxy- phenylboronic acid:aryl halide stoichiometry.

High throughput bulk experimentation: High-throughput experiments of palladium catalyzed S-M reactions were performed in 96-well parallel synthesis metal block assemblies (Analytical Sales and Services, Inc., Flanders, NJ). The reaction mixtures in each glass vial insert of the 96-well metal block were prepared using a Beckman Coulter FX liquid handling robot. 4-Hydroxyphenylboronic acid (**1**, 400 mmol) and aryl halide (**2**–**12**, 400 mmol) in EtOH were pipetted via the Span 8 arm into a master plate and then distributed equally into another set of three 96-well plates using the 96-tip head. A master plate was made containing nine different ratios of boronic acid, **1**, and aryl halide **2**–**12**. Next, DBU (800 mmol) was dispensed separately into each plate followed by XPhosPdG3 (40 mmol) solutions in EtOH using the 96-tip head. The top of the metal block was pressure sealed with a sheet of perfluoroalkoxy (PFA) film and two silicone rubber mats that fully covered the reaction vials. The metal blocks were heated without stirring at 50 °C, 100 °C, 150 °C or 200 °C using a home built block heater for 1 h. Extensive testing revealed that the reactor is sealed well enough to heat above the solvent boiling point with less than 5% solvent loss and no cross talk between wells. After 1 h heating, the plates were cooled to

© 2018 Wiley-VCH Verlag GmbH & Co. KGaA, Weinheim

Table 1. Quantified yields of some S-M microfluidic reactions using HPLC/MS-MS. The same reaction conditions were used in each case (i.e., 200 mmol substrate loading and 1:1 4-hydroxyphenylboronic acid:aryl halide stoichiometry). Peak intensity values are multiples of 1×10^6.

Reaction conditions		13 (1+2)		13 (1+3)		14 (1+4)		15 (1+5)		21 (1+12)	
		Peak intensity	Yield [%]	Peak intensity	Yield [%]	Peak intensity	Yield [%]	Peak intensity	Yield [%]	Peak intensity	Yield [%]
100 °C	0.5 min	1.1	3.4	3.1	13.8	1.3	46.8	0.6	3.5	6.1	23.2
1 °C	1 min	1.1	4.6	3.5	24.5	2.6	54.0	1.6	6.5	4.7	37.7
100 °C	3 min	1.8	6.1	7.6	27.8	3.7	70.9	2.1	15.1	5.1	47.7
100 °C	6 min	5.2	10.5	5.6	48.1	6.1	95.5	4.3	17.6	6.3	48.1
150 °C	0.5 min	2.3	8.0	4.4	48.7	2.8	61.9	1.2	5.6	1.8	45.8
150 °C	1 min	1.6	12.5	2.2	71.2	2.8	93.9	1.1	15.1	2.3	68.6
150 °C	3 min	3.2	35.4	2.8	71.8	3.9	95.6	2	17.1	12.2	70.5
150 °C	6 min	5.3	77.8	7.1	73.1	5.8	97.9	5.2	20.8	6.5	95.6

room temperature, centrifuged, and loaded back onto the deck of the liquid handling robot. Samples for MS autosampling were prepared in 384-well plates by robotic pipetting and diluted by 1000-fold in EtOH. The MS analysis method includes pre-wash and post-wash of the needle to avoid contamination between sample analyses.

Microfluidic experiments: A 1:1 mixture of **1** (400 mmol, 1 equiv) and aryl halide (**2**–**12**, 400 mmol, 1 equiv) in EtOH was loaded into a 1 mL ILS gas tight glass syringe. DBU (800 mmol, 2 equiv) and XPhosPdG3 (2 mmol, 0.5 %) solutions in EtOH were individually loaded into two additional 1 mL ILS gastight glass syringes. Each solution was successively dispensed into the SOR 3225 reactor to engage the reactants. All cross-coupling reactions were run at either 100 °C or 150 °C, with residence times of 0.5, 1, 3, or 6 min unless otherwise noted. The reaction mixtures were collected after quenching and stored at −80 °C. The subsequent ESI-MS and HPLC/MS-MS analyses were performed without further purification.

Acknowledgements

We gratefully acknowledge the financial support from the Department of Defense: Defense Advanced Research Projects Agency (Award no. W911NF-16-2-0020). The efforts of R. Graham Cooks, Ryan Hilger (Amy Facility at Purdue University, Department of Chemistry, heating block fabrication), Tiago J. P. Sobreira, Michael Wleklinski and Andy Koswara are also noted with great appreciation. We also want to thank Shorf Afza for drawing the cover art.

Conflict of interest

The authors declare no conflict of interest.

Keywords: bulk screening · cross-coupling · mass spectrometry · microfluidic evaluation · Suzuki–Miyaura

[1] J. A. Selekman, J. Qiu, K. Tran, J. Stevens, V. Rosso, E. Simmons, Y. Xiao, J. Janey, *Annu. Rev. Chem. Biomol. Eng.* **2017**, *8*, 525 – 547.

[2] a) R. Macarron, M. N. Banks, D. Bojanic, D. J. Burns, D. A. Cirovic, T. Garyantes, D. V. S. Green, R. P. Hertzberg, W. P. Janzen, J. W. Paslay, U. Schopfer, G. S. Sittampalam, *Nat. Rev. Drug Discovery* **2011**, *10*, 188; b) M. Liu, K. Chen, D. Christian, T. Fatima, N. Pissarnitski, E. Streckfuss, C. Zhang, L. Xia, S. Borges, Z. Shi, P. Vachal, J. Tata, J. Athanasopoulos, *ACS Comb. Sci.* **2012**, *14*, 51 – 59.

[3] a) P. Chen, *Angew. Chem. Int. Ed.* **2003**, *42*, 2832 – 2847; *Angew. Chem.* **2003**, *115*, 2938 – 2954; b) A. B. Santanilla, E. L. Regalado, T. Pereira, M. Shevlin, K. Bateman, L.-C. Campeau, J. Schneeweis, S. Berritt, Z.-C. Shi, P. Nantermet, Y. Liu, R. Helmy, C. J. Welch, P. Vachal, I. W. Davies, T. Cernak, S. D. Dreher, *Science* **2015**, *347*, 49 – 53.

[4] a) K. Troshin, J. F. Hartwig, *Science* **2017**, *357*, 175 – 181; b) M. Wleklinski, B. P. Loren, C. R. Ferreira, Z. Jaman, L. Avramova, T. J. P. Sobreira, D. H. Thompson, R. G. Cooks, *Chem. Sci.* **2018**.

[5] a) H. Kim, K. I. Min, K. Inoue, D. J. Im, D. P. Kim, J. Yoshida, *Science* **2016**, *352*, 691 – 694; b) D. R. Snead, T. F. Jamison, *Angew. Chem. Int. Ed.* **2015**, *54*, 983 – 987; *Angew. Chem.* **2015**, *127*, 997 – 1001.

[6] D. Perera, J. W. Tucker, S. Brahmbhatt, C. J. Helal, A. Chong, W. Farrell, P. Richardson, N. W. Sach, *Science* **2018**, *359*, 429 – 434.

[7] C. Len, S. Bruniaux, F. Delbecq, V. Parmar, *Catalysts* **2017**, *7*, 146.

[8] a) C. E. Falcone, Z. Jaman, M. Wleklinski, A. Koswara, D. H. Thompson, R. G. Cooks, *Analyst* **2017**, *142*, 2836 – 2845; b) B. P. Loren, M. Wleklinski, A. Koswara, K. Yammine, Y. Hu, Z. K. Nagy, D. H. Thompson, R. G. Cooks, *Chem. Sci.* **2017**, *8*, 4363 – 4370; c) H. S. Ewan, K. Iyer, S.-H. Hyun, M. Wleklinski, R. G. Cooks, D. H. Thompson, *Org. Process Res. Dev.* **2017**, *21*, 1566 – 1570; d) M. Wleklinski, C. E. Falcone, B. P. Loren, Z. Jaman, K. Iyer, H. S. Ewan, S.-H. Hyun, D. H. Thompson, R. G. Cooks, *Eur. J. Org. Chem.* **2016**, 5480 – 5484.

[9] S. D. Roughley, A. M. Jordan, *J. Med. Chem.* **2011**, *54*, 3451 – 3479.

[10] a) M. Brambilla, M. Tredwell, *Angew. Chem. Int. Ed.* **2017**, *56*, 11981 – 11985; *Angew. Chem.* **2017**, *129*, 12143 – 12147; b) A. Suzuki, *Angew. Chem. Int. Ed.* **2011**, *50*, 6722 – 6737; *Angew. Chem.* **2011**, *123*, 6854 – 6869; c) A. Chatterjee, T. R. Ward, *Catal. Lett.* **2016**, *146*, 820 – 840.

[11] a) B. J. Reizman, Y.-M. Wang, S. L. Buchwald, K. F. Jensen, *React. Chem. Eng.* **2016**, *1*, 658 – 666; b) T. Noël, A. J. Musacchio, *Org. Lett.* **2011**, *13*, 5180 – 5183; c) T. Noël, S. Kuhn, A. J. Musacchio, K. F. Jensen, S. L. Buchwald, *Angew. Chem.* **2011**, *123*, 6065 – 6068.

[12] a) S. Fukumoto, O. Ujikawa, S. Morimoto, Y. Asano, S. Mikami, N. Tokunaga, M. Kori, T. Imaeda, K. Fukuda, S. Nakamura in Sulfonamide derivative and use thereof, Vol. Google Patents, **2012**; b) S. Fu, W. Xiang, J. Chen, L. Ma, L. Chen, *Chem. Biol. Drug Des.* **2017**, *89*, 815 – 819; c) M. Sánchez-Peris, J. Murga, E. Falomir, M. Carda, J. A. Marco, *Chem. Biol. Drug Des.* **2017**, *89*, 577 – 584; d) V. E. Gregor in Tricyclic compound derivatives useful in the treatment of neoplastic diseases, inflammatory disorders and immunomodulatory disorders, Vol. Google Patents, **2014**; e) M. Sánchez-Peris, E. Falomir, J. Murga, M. Carda, J. A. Marco, *Bioorg. Med. Chem.* **2016**, *24*, 3108 – 3115; f) P. R. D. Murray, D. L. Browne, J. C. Pastre, C. Butters, D. Guthrie, S. V. Ley, *Org. Process Res. Dev.* **2013**, *17*, 1192 – 1208; g) K.-S. Jang, *Mol. Cryst. Liq. Cryst.* **2016**, *633*, 123 – 128.

[13] B. Schmidt, M. Riemer, *J. Org. Chem.* **2014**, *79*, 4104 – 4118.

[14] M. A. Düfert, K. L. Billingsley, S. L. Buchwald, *J. Am. Chem. Soc.* **2013**, *135*, 12877 – 12885.

Manuscript received: March 7, 2018
Revised manuscript received: April 21, 2018
Version of record online: June 19, 2018

© 2018 Wiley-VCH Verlag GmbH & Co. KGaA, Weinheim